THE JOURNAL OF PHYSICAL CHEMISTRY C

ARTICLE

pubs.acs.org/JPCC

Molar Extinction Coefficient of Single-Wall Carbon Nanotubes

Friedrich Schöppler,[†] Christoph Mann,[†] Tilman C. Hain,[†] Felix M. Neubauer,[†] Giulia Privitera,[‡] Francesco Bonaccorso,[‡] Daping Chu,[‡] Andrea C. Ferrari,[‡] and Tobias Hertel*[,†]

[†]Institute of Physical and Theoretical Chemistry, Department of Chemistry and Pharmacy, Julius-Maximilians University of Würzburg, D-97074 Würzburg, Germany

[‡]Department of Engineering, University of Cambridge, Cambridge, CB3 OFA, U.K.

Supporting Information

ABSTRACT: The molar extinction coefficient of single-wall carbon nanotubes (SWNTs) is determined using fluorescence tagging, as well as atomic force microscopy (AFM) imaging, which facilitate the correlation of nanotube concentrations with absorption spectra. Tagging of SWNTs is achieved using fluorescence-labeled single-strand DNA oligomers as the dispersion additive, while AFM imaging is used to determine the mass of SWNTs in the retentate of vacuum-filtered colloidal SWNT suspensions. The resulting absorption cross section for the first exciton transition of (6,5) nanotubes of 1.7×10^{-17} cm^2 per C-atom corresponds to an extinction coefficient of (4400 ± 1000) M$^{-1}\cdot$cm^{-1}, which is equivalent to an oscillator strength of 0.010 per carbon atom.

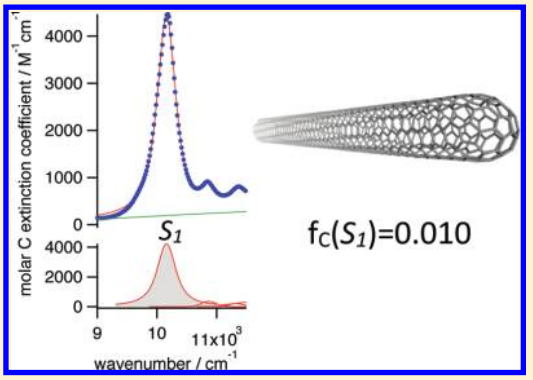

INTRODUCTION

The concentration of nanoparticles in suspensions is crucial for many kinetic phenomena with chemical or photophysical nature, but the measurement of particle concentrations is often fraught with large and undesirable uncertainties. In contrast, absorption cross sections and the corresponding molar extinction coefficients of molecular systems are generally better known and allow a reliable determination of molecular concentrations in solutions. Moreover, the oscillator strength of optical transitions—closely related to the extinction coefficient and frequently just as poorly characterized for nanoparticle systems—represents one of the most fundamental characteristics of optically active systems and allows key insights into the character of excited states. As a consequence, extinction coefficients and oscillator strengths of nanomaterials are often debated, due to inherent difficulties with the determination of nanoparticle concentrations in suspensions.

Here, we use fluorescence labeling and atomic force microscopy (AFM) for the determination of single-wall carbon nanotube (SWNT) concentrations in aqueous suspension. A comparison with previously published data suggests that some studies may have overestimated SWNT concentrations by up to a factor of 30.[1−6] A measurement of the absorption cross section with greater confidence is thus clearly desirable, particularly since it is also essential for the determination of other photophysical properties such as exciton size[7] or diffusion coefficients.[8] Comparative studies of photoluminescence (PL) action cross sections—a product of absorption cross section and PL quantum yield (QY)—would also benefit from greater confidence regarding the magnitude of absorption cross sections.[9]

The first reports of SWNT absorption cross sections by Islam et al. cited 0.08×10^{-17} cm^2 per C-atom for the second sub-band S_2 transitions.[1] However, the samples used in that study were most likely heavily aggregated[10,11] and spectrally congested, which makes a determination of oscillator strengths difficult. Another study using DNA-suspended and (6,5) enriched SWNTs by Zheng et al. gives an absorption cross section for first sub-band S_1 excitons of 0.7×10^{-17} cm^2 per C-atom.[2] A recent Rayleigh scattering investigation finds an S_2 cross section of 2.5×10^{-17} cm^2 per C-atom.[6] As a side note, we recall that at normal incidence graphene is known to absorb 2.3% per layer in the same spectral range as the S_1 exciton feature of (6,5) SWNTs studied here.[12,13] This corresponds to a photoabsorption cross section of 0.6×10^{-17} cm^2 per C-atom.

In the following, we discuss the determination of SWNT exciton absorption cross sections using two independent techniques for the assessment of nanotube concentrations: (1) fluorescence labeling and (2) AFM imaging of vacuum filtered SWNT retentate. In addition, and in contrast to several previous studies of absorption cross sections,[1−6] the SWNTs used for our investigations are isolated monomers and highly (6,5) enriched to avoid ambiguities with the interpretation of congested spectra.

Received: June 6, 2011
Published: June 22, 2011

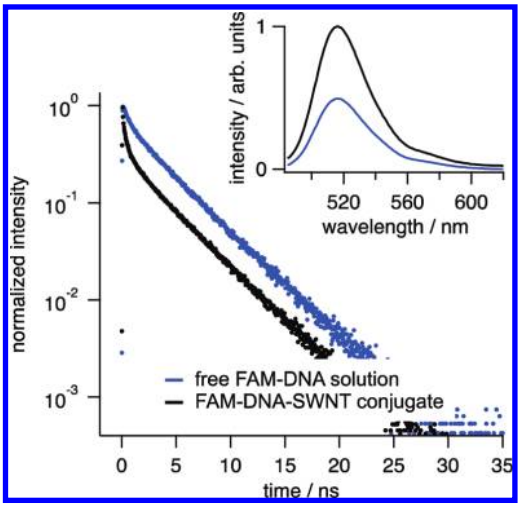

Figure 1. Time-resolved fluorescence spectra of a fluorophore FAM-DNA solution and of FAM-DNA-SWNT conjugates. Emission from the adsorbed FAM-DNA is found to be less efficient than for the free fluorophore. The inset shows emission spectra of free and surface-bound FAM-DNA for determination of the concentration of adsorbed DNA in the nanotube suspension.

EXPERIMENTAL SECTION

For fluorescence labeling experiments we use 6-carboxyfluorescein (FAM)-labeled single-strand DNA of the $(GT)_{n=16}$ type (FAM-DNA). One milligram of SWNT soot from the CoMoCAT process[14] is dispersed in 3 mL of phosphate-buffered saline (PBS) HPLC water by ultrasonication with 16 μM FAM-DNA oligomer solution. The resulting dark suspension is ultracentrifuged for 18 h at 288 000g in a density gradient[15] in order to sort nanotubes by diameter, as well as to remove nanotube aggregates, residual catalyst, and other contaminants.[10] SWNT fractions are filtered 20 times with centrifugal filters (Amicon Ultra, Millipore) to remove any excess of free FAM-DNA. The absorption spectrum of the resulting purple suspension is dominated by the S_1 and S_2 exciton transitions of the (6,5) SWNT at 991 and 575 nm,[16] respectively (see Supporting Information (SI)). Assuming similar absorption cross section for different chiralities, the relative abundance of the (6,5) species is estimated to be about 85−90% of all semiconducting nanotubes.

RESULTS AND DISCUSSION

Fluorescence spectra of a 5.0 nM suspension of free FAM-DNA oligomer and of a SWNT sample with SWNT-bound FAM-DNA are shown in the inset of Figure 1. A comparison of integrated PL intensities of the free FAM-DNA solution with FAM-DNA-SWNT conjugates allows us to determine the FAM-DNA concentration in the SWNT suspension if differences in PL QY are taken into consideration. In Figure 1 we also reproduce time-correlated single photon counting traces from both free and SWNT-bound FAM-DNA. These allow us to account for changes of the PL QY when calculating FAM-DNA-SWNT conjugate concentrations. The PL decay of adsorbed FAM-DNA is found to be biexponential—in agreement with previous investigations[17]—with an average lifetime of 0.68 ns, while the free fluorophore decays with an average lifetime of 1.72 ns. This corresponds to a 61% decrease of the PL QY of the adsorbed fluorophore with respect to the free fluorophore. For the

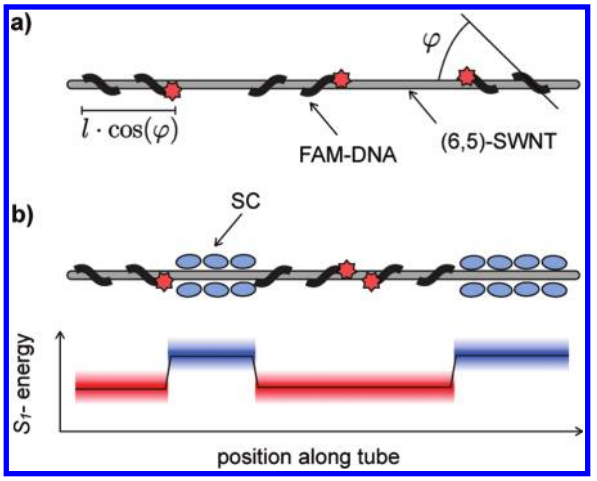

Figure 2. (a) Schematic illustration of a partially DNA-covered nanotube. (b) Absorption of excitons in regions covered by DNA oligomers, and those accessible to anionic surfactant, such as SC, are characterized by slightly different center wavelengths. This is used to assess the degree of SWNT saturation with DNA from optical absorption spectra.

FAM-DNA-SWNT conjugate sample in Figure 1, this yields a concentration of surface-bound FAM-DNA of 24 nM.

For the conversion of the concentration of adsorbed FAM-DNA to a SWNT concentration, we need to determine the DNA-SWNT stoichiometry, as given by the DNA number density ρ per tube unit length. The latter is related to θ, the fraction of the tube surface covered by DNA, the wrapping angle φ between DNA strand orientation and the tube axis, and the DNA oligomer length l by $\rho = \theta/(l \cdot \cos(\varphi))$ (see SI). Molecular dynamics calculations for a (11,0) SWNT indicate that the helical pitch of DNA wrapped around SWNTs is constrained by steric and Coulomb interactions and by the flexibility of the DNA backbone and lies between 8 and 10 nm, corresponding to wrapping angles of 25° and 30°, respectively.[18] In combination with the range of anticipated phosphor−phosphor distances of 0.56−0.70 nm in the DNA backbone,[18−20] this suggests that adsorbed $(GT)_{n=16}$ will cover a region on the tube surface $l \cdot \cos(\varphi)$ between 16 and 20 nm in length. Due to steric constraints, it is unlikely that more than one DNA strand can bind to the same segment of a small diameter SWNT.[18]

The coverage θ needs to be assessed independently. Here, this is done experimentally using frequency shifts of the S_1 exciton caused by adsorption of an anionic surfactant (sodium cholate, SC) on bare nanotube sections. These frequency shifts—on the order of a few nanometers—can be analyzed using a heterogeneous adsorption model (see Figure 2 and SI). First, the absorption wavelengths of density gradient ultracentrifugation (DGU)-enriched, purely DNA-covered, and purely SC-covered surfaces of λ_{DNA} = 991 nm and λ_{SC} = 982 nm, respectively, are measured independently. To first order, the exciton peak position λ_{expt} after addition of SC to a DNA-SWNT conjugate suspension is then given by linear interpolation of the known absorption wavelengths of the pure phases in the ternary DNA-SC-H_2O system (see SI). Here this interpolation is done using the arithmetic mean of the exciton transitions in the pure phases, and we have $\lambda_{expt} = \theta\lambda_{DNA} + (1 - \theta)\lambda_{SC}$. If 2 wt % SC is added to a freshly prepared and ultracentrifuged DNA-SWNT conjugate suspension, we find a strong blue-shift upon SC addition from 991 to 984 nm, indicating that only a fraction of the tubes

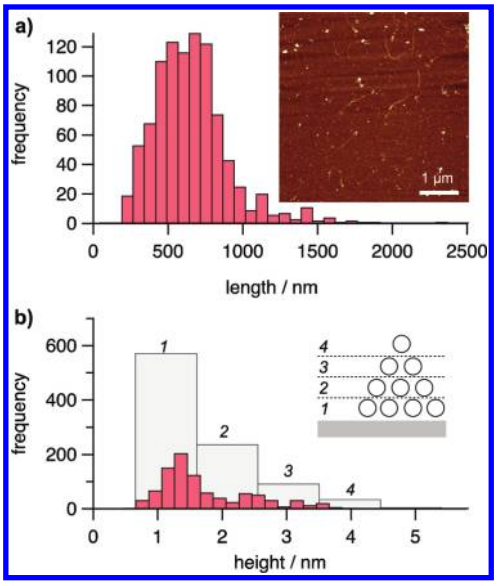

Figure 3. (a) Aggregate length and (b) height histograms obtained from the structures found in 38 AFM images of sparse retentates. The inset in panel a shows an AFM image of a sparse SWNT retentate after transfer from a cellulose filter membrane to a Si substrate.

(~20%) is covered with DNA after DGU. This is in good agreement with published estimates of ~25%.[21] If the freshly prepared DNA-SWNT suspension is saturated after fractionation by the addition of excess DNA, the absorption wavelength is slightly shifted to 989 nm, indicating that the DNA coverage in this case is ~80%.

The resulting absorption cross section for DNA suspended SWNTs then becomes $(2.3 \pm 0.7) \times 10^{-17}$ cm^2 per C-atom (see SI). The largest uncertainty of about 30% here arises from the determination of the DNA surface coverage.

Next we use AFM imaging of the retentate from vacuum filtered SWNT suspensions to determine SWNT concentrations. Here, SWNT suspensions are prepared by DGU with SC and sodium dodecyl sulfate (SDS) surfactant mixtures.[10,11,22] The resulting (6,5) enriched suspensions are diluted with surfactant solution to an optical density (OD) in the S_1 transition range of about 10^{-4}. One milliliter of the diluted suspension then undergoes vacuum filtration through cellulose filters with 0.1 μm pore size. The briefly dried retentate is washed with deionized (DI) water before being transferred to Si substrates for AFM investigation (see SI).

AFM images from sparsely SWNT-covered Si surfaces, such as in Figure 3, reveal that the filtration process yields both individual and aggregated SWNTs. The AFM images are used to measure the length and center height of single tubes, tube aggregates, or aggregate sections. This allows us to determine the total volume of SWNTs in the retentate. For the calculation of aggregate volume, we assume close packing, with a lattice constant of 1.1 nm, and nearly spherical aggregate cross sections. Considering a variety of aggregate geometries then yields the following estimate of height-to-aggregate size relationships: 0.62−1.58 nm: 1.5 tubes; 1.59−2.53 nm: 4.2 tubes; 2.54−3.48 nm: 7.2 tubes; 3.49−4.33 nm: 11.5 tubes (see Figure 3). The average tube number per aggregate is expected to be slightly smaller since aggregates tend to taper off toward their ends, whereas our calculation assumes a homogeneous aggregate diameter over the measured segments. The absorption

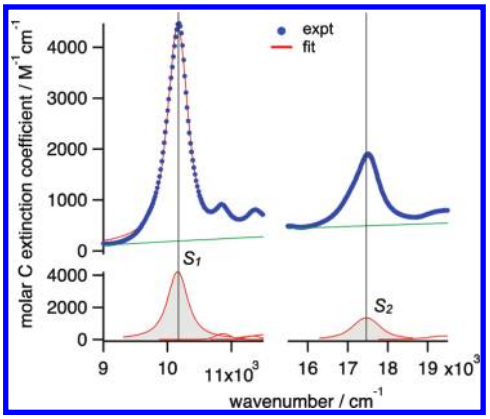

Figure 4. Calibrated absorption spectra of a (6,5) enriched SWNT suspension. The oscillator strengths of the S_1 and S_2 transitions are obtained from integration over the Voigt profiles in the lower part of the figure.

cross section, σ, is then determined from the OD of the filtered sample volume V_S and the length d of the optical path in the spectrometer cell:

$$\sigma = \frac{\mathrm{OD}V_s \ln(10)}{88\ \mathrm{nm}^{-1} N_T L_T d}$$

where the product of the number and length of tubes, N_T and L_T, with 88 nm^{-1} corresponding to the number of atoms in the suspension (88 is the number of carbon atoms per nm length of a (6,5) SWNT). From the average of over 38 AFM images with 25 μm^2 area each, and with a total of 952 single tubes or tube aggregates, we obtain an absorption cross section of the S_1 exciton in SC suspension of 1.1×10^{-17} cm^2, with an estimated uncertainty of 20%.

Unfortunately, the two absorption cross sections obtained from fluorescence labeling and AFM imaging experiments do not fall within their respective margins of error. This suggests that some systematic and perhaps some statistical uncertainties are unaccounted for by the error analysis. Without a better understanding of the origin of these uncertainties, however, we cannot give preference to either of the two values and in the following discussion will thus use the average cross section of 1.7×10^{-17} cm^2 per C-atom. On the basis of the variation of our results for different preparation runs and samples, we estimate that the uncertainty associated with this value is $\sim 0.4 \times 10^{-17}$ cm^2 per C-atom. Other sources of uncertainty could be a possible overestimation of the DNA coverage on SWNT surfaces in the fluorescence labeling experiments, or a possible loss of SWNT material during sample transfer to the Si substrate for the AFM study. For both experiments, this would imply that the measured cross section represents an upper bound. As discussed further below, we will show that the value is in good agreement with expectations based on theoretical predictions of the exciton size.

The absorption cross section is used to calculate the molar extinction coefficient of (6,5) SWNTs at the maximum of the S_1 exciton of 4400 M$^{-1}\cdot$cm^{-1}. Integration over the S_1 and S_2 exciton absorption features shown in Figure 4 then yields transition strengths of 2.4×10^9 mol$^{-1}\cdot$cm and 1.4×10^9 mol$^{-1}\cdot$cm, respectively (M$^{-1}\cdot$cm^{-1} = L$\cdot$mol$^{-1}\cdot$cm^{-1} = 1000 cm$^2\cdot$mol^{-1}). These integrals can be used to calculate the oscillator strength of

the corresponding transitions from[23,24]

$$f = \frac{4\varepsilon_0 c^2 m_e \ln(10)}{N_A e_0^2} \int \varepsilon(\tilde{\nu})\, d\tilde{\nu}$$

where ε_0 is the free space permittivity, c is the speed of light, m_e is the electron mass, N_A is Avogadro's number, e_0 is the elementary charge, $\varepsilon(\tilde{\nu})$ is the molar extinction coefficient, and $\tilde{\nu}$ is the wavenumber (in cm^{-1}).[23] The constants leading the integral become 4.319×10^{-12} mol·cm^{-1}. The resulting oscillator strengths per C-atom are 0.010 and 0.006 for the S_1 and S_2 exciton transitions, respectively. In combination with the transition line width, Δ_{fwhm}, this can also be used to establish a convenient relationship between c_C, the carbon atom concentration in suspension (in mol/L), and the OD of the S_1 transition according to:

$$c_C = B\frac{\Delta_{fwhm} OD}{fd}$$

where d is the thickness of the optical cell and f is the the C-atom oscillator strength. For convenience, the constant $B = 5.1 \times 10^{-8}$ mol·L^{-1}·cm·nm^{-1} is calculated for the use with units typically utilized in the lab, i.e., the fwhm is given in nanometers, and the spectrometer cell thickness is given in centimeters. Care needs to be taken to ensure that the measurement of the fwhm is not affected by spectral congestion. In addition, one needs to bear in mind that oscillator strengths may depend to a varying degree on solvent, surfactant, possible tube filling, and the state of aggregation.

The exciton oscillator strengths and absorption cross sections determined above are larger than most previous estimates with values ranging from 2.9×10^{-18} cm^2 to 0.7×10^{-17} cm^2 per C-atom for the S_1[2,5] and from 2.4×10^{-19} cm^2 to 0.5×10^{-17} cm^2 per C-atom for the S_2 transition.[1,3,4] All values are here adjusted for irradiation with unpolarized light, which is equivalent to irradiation of randomly oriented nanotubes with linearly polarized light. If the exciting light is polarized in the direction of the transition dipole parallel to the nanotube axis, these absorption cross sections have to be multiplied by a factor of 2. The results presented here provide a new determination of absorption cross sections that benefits from the use of highly enriched nanotube samples with little or no spectral congestion as well as from the use of two independent approaches for the determination of SWNT concentrations, with similar results obtained for both types of experiments.

In addition to providing a useful means for the determination of nanotube concentrations in aqueous suspensions from absorption spectra, these results also allow an assessment of exciton size using the relationship between absorption oscillator strength and radiative lifetimes. Without knowledge of the concentration of a solution, its OD generally allows the determination of the total absorption cross-section and, in combination with the transition line width, the total oscillator strength of a system. If the fluorophore concentration is known, one can use this for a calculation of the fluorophore oscillator strength as well as the corresponding radiative lifetime τ_{rad} using[23,24]

$$\frac{1}{\tau_{rad}} = A_{ab} = \frac{2\pi e_0^2 n^2}{\varepsilon_0 m_e c \lambda^2}\frac{g_a}{g_b} f$$

Here $n = 1.33$ is the refractive index of water at 982 nm and g_a and g_b are the ground and excited state degeneracies. We use the radiative exciton lifetime of (1.6 ± 0.3) ns[25] to reverse this argument and estimate the fluorophore concentration from the total oscillator strength. From the above radiative exciton lifetime we obtain an S_1 oscillator strength of 5. The oscillator strength of 0.010 on a per-atom basis thus suggests that 500 C-atoms contribute to the coherent exciton oscillation. For the (6,5) tube with 88 C-atoms per nanometer length, and using a Gaussian exciton envelope function,[26] with $\psi(z_e, z_h) \propto \exp(-(z_e - z_h)^2/2s^2)$, this yields an electron−hole correlation length s of $(500/88)/\sqrt{\pi}$ nm = 3.2 nm, in good agreement with previously measured and calculated exciton sizes ranging from 2.0 nm to ∼3 nm.[7,26,27] In fact, this underlines that the above S_1 oscillator strength is consistent with the current theoretical understanding of the nature and properties of SWNT excitons.

CONCLUSION

We estimated the molar extinction coefficients and oscillator strengths of the S_1 exciton in (6,5) SWNTs using two different approaches for determining carbon nanotube concentrations in colloidal suspensions. One approach is based on fluorescence labeling, while the other one makes use of AFM imaging of vacuum filtered SWNTs on a Si wafer. The results allow to determine the molar C extinction coefficient of the S_1 exciton in (6,5) SWNTs of (4400 ± 1000)·M^{-1}·cm^{-1}, which corresponds to a C absorption cross section of $(1.7 \pm 0.4) \times 10^{-17}$ cm^2 or an oscillator strength of 0.010. This oscillator strength can be used in combination with the previously measured radiative S_1 lifetime of 1.6 ns for a new determination of the S_1 exciton size of (6,5) SWNTs of 3.2 nm, which is confirmed by previous experimental and theoretical studies.

ASSOCIATED CONTENT

Supporting Information. Absorption spectra of DGU enriched DNA-FAM-SWNT samples; geometrical considerations for determination of the length of a SWNT segment covered by a single-strand DNA oligomer; DNA coverage; optical absorption and absorption cross section; vacuum filtration; and AFM characterization. This material is available free of charge via the Internet at http://pubs.acs.org.

AUTHOR INFORMATION

Corresponding Author
*E-mail: tobias.hertel@uni-wuerzburg.de.

ACKNOWLEDGMENT

F.B. acknowledges funding from a Newton International Fellowship. A.C.F. acknowledges funding from the ERC grant NANOPOTS, a Royal Society Brian Mercer Award for Innovation, and a Royal Society Wolfson Research Merit Award.

REFERENCES

(1) Islam, M. F.; Milkie, D. E. C.; Kane, L.; Yodh, A. G.; Kikkawa, J. M. *Phys. Rev. Lett.* **2004**, *93* (3), 037404.
(2) Zheng, M.; Diner, A. *J. Am. Chem. Soc.* **2004**, *126*, 15490.
(3) Schneck, J. R.; Walsh, A. G.; Green, A. A.; Hersam, M. C.; Ziegler, L. D.; Swan, A. K. *J. Phys. Chem. A*, **2011**, *115*, 3917.
(4) Berciaud, S.; Cognet, L.; Lounis, B. *Phys. Rev. Lett.* **2008**, *101* (7), 077402–1.
(5) Carlson, L. J.; Maccagnano, S. E.; Zheng, M.; Silcox, J.; Krauss, T. D. *Nano Lett.* **2007**, *7* (12), 3698.

(6) Joh, D. Y.; Kinder, J.; Herman, L. H.; Ju, S. Y.; Segal, M. A.; Johnson, J. N.; Chan, G. K. L.; Park, J. *Nat. Nanotechnol.* **2011**, *6*, 51.
(7) Luer, L.; Hoseinkhani, S.; Polli, D.; Crochet, J.; Hertel, T.; Lanzani, G. *Nat. Phys.* **2009**, *5*, 54.
(8) Wang, F.; Dukovic, G.; Brus, L. E.; Heinz, T. F. *Science* **2005**, *308*, 838.
(9) Tsyboulski, D. A.; Rocha, J. R.; Bachilo, S. M.; Cognet, L.; Weisman, R. *Nano Lett.* **2007**, *7* (10), 3080.
(10) Crochet, J.; Clemens, M.; Hertel, T. *J. Am. Chem. Soc.* **2007**, *129* (26), 8058.
(11) Bonaccorso, F.; Hasan, T.; Tan, P. H.; Sciascia, C.; Privitera, G.; Di Marco, G.; Gucciardi, P. G.; Ferrari, A. C. *J. Phys. Chem. C* **2010**, *114*, 17267.
(12) Mak, K. F.; Sfeir, M. Y.; Wu, Y.; Lui, C. H.; Misewich, J. A.; Heinz, T. F. *Phys. Rev. Lett.* **2008**, *101*, 196405.
(13) Nair, R. R.; Blake, P.; Grigorenko, A. N.; Novoselov, K. S.; Booth, T. J.; Stauber, T.; Peres, N. M. R.; Geim, A. K. *Science* **2008**, *320*, 1308.
(14) Kitiyanan, B.; Alvarez, W. E.; Harwell, J. H.; Resasco, D. E. *Chem. Phys. Lett.* **2000**, *317*, 497.
(15) Arnold, M. S.; Stupp, S. I.; Hersam, M. C. *Nano Lett.* **2005**, *5*, 713.
(16) Weisman, R. B.; Bachilo, S. M. *Nano Lett.* **2003**, *3* (9), 1235.
(17) Alvarez-Pez, J. M.; Ballesteros, L.; Talavera, E.; Yguerabide, J. *J. Phys. Chem. A* **2001**, *105*, 6320.
(18) Johnson, R. R.; Johnson, A. T. C.; Klein, M. L. *Nano Lett.* **2008**, *8* (1), 69.
(19) Manohar, S.; Tang, T.; Jagota, A. *J. Phys. Chem. C* **2007**, *111*, 17835.
(20) Manohar, S.; Mantz, A. R.; Bancraft, K. E.; Hui, C.; Jagota, A.; Vezenov, D. V. *Nano Lett.* **2008**, *8* (12), 4365.
(21) Jeng, E. S.; Moll, A. E.; Roy, A. C.; Gastala, J. B.; Strano, M. S. *Nano Lett.* **2006**, *6* (3), 371.
(22) Arnold, M. S.; Green, A. A.; Hulvat, J. F.; Stupp, S. I.; Hersam, M. C. *Nat. Nanotechnol.* **2006**, *1*, 60.
(23) Strickler, S. J.; Berg, R. A. *J. Chem. Phys.* **1962**, *37* (4), 814.
(24) Lewis, G. N.; Kasha, M. *J. Am. Chem. Soc.* **1945**, *67*, 994.
(25) Hertel, T.; Himmelein, S.; Ackermann, T.; Stich, D.; Crochet, J. *ACS Nano* **2010**, *4*, 7161.
(26) Capaz, R. B.; Spataru, C. D.; Beigi, S. I.; Louie, S. G. *Phys. Rev. B* **2006**, *74*, 121401(R).
(27) Perebeinos, V.; Tersoff, J.; Avouris, P. *Phys. Rev. Lett.* **2004**, *92*, 257402.